Military Technical College
Kobry El-Kobbah,
Cairo, Egypt

14th International Conference on Applied Mechanics and Mechanical Engineering.

Dump combustor swirling flow reconstruction using neural network

By

Saad Ahmed* Hany El Kadi*

Abstract:

Knowledge of continuous evolution of fluid flow characteristics is very useful and essential for better designs of efficient combustors. Many experimental techniques such as Laser Doppler Velocimetry (LDV) measurements provide only limited discrete information at given points; especially, for the cases of complex flows such as swirling flows of dump combustors. For these types of flows, usual numerical interpolating schemes appear to be unsuitable. Artificial Neural Network (ANN) methods are thus proposed and their results are presented in this paper and are compared with the experimental data used for training purposes. This pilot study showed that ANN is an appropriate method for predicting swirl flow velocity in a model of a dump combustor. In summary, this detailed information is fundamental for better designs and optimization of dump combustors.

Keywords:

Swirl flow, dump combustors and neural network.

* Mechanical Engineering Department, College of Engineering, American University of Sharjah, Sharjah, PO Box 26666, UAE.

1. Introduction:

Turbulent swirling flows have been and continue to be of considerable interest to both engineers and scientists. The designers of combustion chambers have used swirl to promote rapid mixing of fuel and oxidizer. Swirling flows can cause a flow reversal that entrains and recirculates a portion of the hot combustion products to mix with the incoming air and fuel, thereby, maintaining combustion. This recirculation combined with the enhanced mixing caused by the swirl induced turbulence can lead directly or indirectly to one or more of the following: (a) increased combustion efficiency; (b) reduced emissions (NOx, soot, unburnt hydrocarbons); (c) reduced flame length and thereby smaller combustors; (d) improved stability; (e) uniform pattern factor (leading to increased turbine life); and (f) improved blow-off limits.

For an analysis of combustion processes, one requires a broad knowledge of interrelated subjects such as injection, atomization and mixing, flow separation and recirculation, ignition, combustion, and heat release. This has made realistic simulation and solution of swirling recirculating turbulent flows a difficult and a challenging task. A considerable number of attempts have been made to model turbulent reacting and non-reacting swirling flows. So far, the efforts have not been always successful. This is due to the problems associated with closure models representing turbulence and chemical reaction. It is generally agreed that the impediments to the development of a mathematical model for flows of engineering interest are the lack of in-depth understanding of turbulence and the applications of inadequate physical models. Today, one of the most commonly used turbulence models for representing isothermal flows is the two-equation model. For combusting flows, derivatives of the isothermal physical models are used, which may include a simple representation of flame-turbulence interaction. These models have been successful in the simulation of a few relatively simple isothermal and combusting turbulent flows. However, experiments and calculations of the exchange coefficients from mean value distributions have shown that, for swirling flows, the turbulent stress distributions are anisotropic and the extension of closure models based on uniform transport mechanisms most often fail to predict the flowfield accurately. Currently, computational fluid dynamics (CFD) codes suffer from the lack of a proper validation procedure; complementary detailed experimental and analytical studies must be pursued to strengthen combustor design methodology based on CFD (see references 1-6). Consequently, a considerable aid to the development of mathematical modeling is the creation of an extensive detailed experimental database which can be used for validations of numerical codes.

This paper reports on the isothermal measurements which are designed to address the turbulence modeling problem. There are two problems: (i) the obtained velocity-field is not continuous, (ii) the acquisition area remains limited and a complete investigation of the flow-field would request numerous measurement areas. Thus, an experimental investigation can require a very long time to obtain a sufficient amount of data. Because neural networks can express nonlinearities, they seem to be an efficient tool for the reconstruction of data linked to multiple parameters, and thus an interesting alternative solution to common interpolation schemes. To evaluate the accuracy of this ANN technique, a large set of data has first been measured using LDV technique. Next, the set has been divided into two parts: the first being used by the neural network in order to reconstruct the velocity-field during the learning step, and the second to estimate the reconstruction efficiency by comparing values obtained with the neural method to experimental measurements.

Detailed knowledge of confined swirling flows/flames is required for proper design and performance control of gas turbine and ramjet combustors. The majority of the research to date has the common goal of increasing the understanding of such complex flowfields and improving the accuracy of the computational methods in an effort to reduce the expensive cut-and-try approach to combustor design (see references 1-6).
The complete mapping of a swirl stabilized combustion chamber, based upon comprehensive and detailed measurements of fluctuating components of velocity, temperature, species concentrations and their correlations are few. Such data sets would allow the testing of turbulence and combustion models, which are necessary to solve the averaged conservation equations. However, gas turbine combustors are geometrically complex with many unknown flows through cooling slots and dilution holes. Ideally, one would like to take measurements in a three- dimensional combustor, but this is too complicated. Some combustor features such as the influence of swirl are best studied in axisymmetric systems requiring fewer measurements. Such a system is employed in this investigation.

2. Experimental Facility:

2.1 Modular research combustor

The most important design criterion was the simultaneous requirement of preserving the integrity of the axisymmetric flow field and providing excellent optical access for two-component fiber-optic LDV. To satisfy this criterion, a modular research combustor which consisted of two major sections namely an inlet assembly, and a combustion chamber was designed and fabricated.

2.1.1 Inlet assembly

The inlet assembly consisted of a 300 mm diameter settling chamber, a Plexiglas inlet pipe [2850 mm in length and 101.6 mm inner diameter (ID)], and a cylindrical Teflon swirler housing [104.5 mm (ID), 152.4 mm outer diameter (OD), and 154 mm in length]. A transition section which enabled the swirler to be mounted was incorporated in this housing. A unique feature of the design was the capability of positioning the dump plane (swirler housing) relative to the measurement station in the combustion chamber, see Fig. 1. This was accomplished by supporting the entire inlet assembly on a traversing mechanism controlled by a stepping motor. Throughout these experiments, the inlet average velocity (assuming simple plug flow across the pipe) was monitored with a flow meter located far upstream of the swirler housing, and was maintained at an average velocity of U_o = 16 + 0.4 m/s, corresponding to a Reynolds number (Re = □ U_o x swirler OD /□)of 1.5 x 10^5. This velocity was large enough to ensure turbulent flow in the combustor.

Figure (1): Schematic of the dump combustor model

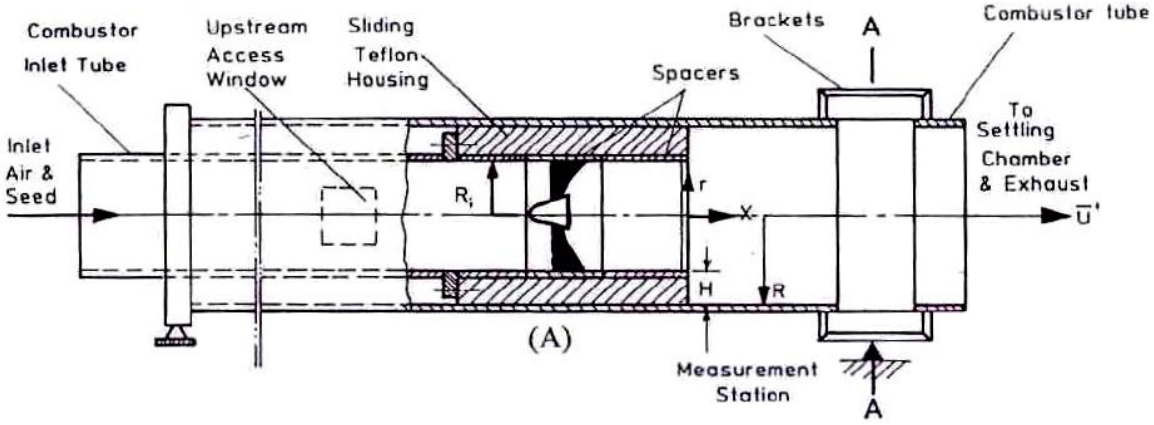

2.1.2 Combustion chamber

This section consisted of a Plexiglas tube (152.4 mm ID and 1850 mm in length) terminating into a larger pipe (exhauster). The measurement station was designed to accept different window assemblies. One was designed to provide optical access for traversing in the horizontal plane along the combustor diameter. By traversing a two-component LDV system in the horizontal plane, U and W components of the velocity vector can be realized, see Fig 1

2.1.3 Swirler design

The swirler is a free vortex swirler and is similar to the one used by Ahmed and Nejad [10]. The current facility employed a swirler which has 12 curved vanes. Swirler dimensions are 19 mm ID (central hub) and 101.6 mm OD.

2.2 Laser velocimeter

Velocity measurements were performed with a TSI Inc. 9100-7 four-beam, two-color, back scatter fiber-optic LDV system. This system was equipped with two TSI 9180-3A frequency shifters to provide directional sensitivity. The entire optics were mounted on a three-axis traversing table with a resolution of ±2.5 □**m.** Some of the features of the optical set-up were as follows: 1. The system was configured so that the fringe inclinations were at 45.67^{o} and 135.17^{o} to the combustor centerline. 2. The approximate measurement volume dimensions based on $1/e^2$ intensity points were 390 □m length and 60 □m diameter.

2.3 Data acquisition and analysis

The photomultipliers signals were processed by two TSI burst counters - models 1990 B\C with low pass filters, set at 20 MHz, and high pass filters set at 100 MHz on each processor. Calculations of statistical moments from standard formulae were done at each measurement location using double precision data (48 bit), see Ahmed and Nejad [6].

2.4 Artificial neural network

Artificial neural networks have emerged as one of the useful artificial intelligence concepts used in the various engineering applications. Due to their massively parallel structure and

ability to learn by example, ANN can deal with nonlinear modeling for which an accurate analytical solution is difficult to obtain. ANN has already been used in medical applications, image and speech recognition, classification and control of dynamic systems, among others; but only recently have they been used in swirl flow velocity field reconstruction [7 & 8].

ANN can generally be defined as a structure composed of a number of interconnected units [9]. Each unit has an input/output (I/O) characteristic and implements a local computation or function. The output of each unit is determined by its I/O characteristic, its interconnection to other units and (possibly) external inputs, as well as its internal function. The network usually develops an overall functionality through one or more forms of training. The fundamental unit or building block of the ANN is called neuron [10]. The neuron has a set of inputs (X_i) weighted before reaching the main body of the processing element. In addition, it has a bias term, a threshold value that has to be reached or exceeded for the neuron to produce a signal, a nonlinearity function (f_i) that acts on the produced signal (R_i), and an output (O_i).

Learning is the process by which the neural network adapts itself to a stimulus and eventually (after adjusting its synaptic weights) produces the desired response. ANN generally consist of a number of layers: the layer where the input patterns are applied is called the input layer, the layer where the output is obtained is the output layer, and the layers between the input and output layers are the hidden layers (Fig. 2). There may be one or more hidden layers, which are so named because their outputs are not directly observable. The addition of hidden layers enables the network to extract higher-order statistics which is particularly valuable when the size of the input layer is large [15]. Many publications discuss the development and theory of ANN (for example, see references [9-11]).

The back-propagation training algorithm [9 &10] is commonly used to iteratively minimize the following cost function with respect to the interconnection weights and neurons thresholds:

$$E = \frac{1}{2}\sum_{1}^{P}\sum_{i=1}^{N}(d_i - O_i)^2 \tag{1}$$

Where P is the number of training input/output patterns and N is the number of output nodes. d_i and O_i are the target and actual responses for output node *i* respectively. Iteratively, the interconnection weights between the j^{th} node and the i^{th} node are updated as:

$$w_{ji}(t+1) = \alpha \; w_{ji}(t) + \eta \; x_i \; f'\left(net_j^k\right) \sum_{l=1}^{N}\left(d_l - O_l\right) \; f'\left(net_l^0\right) \; w_{lj} \tag{2}$$

Where α is a momentum constant, η the learning rate, x_i the input pattern at the iterative sample *t*, net^0_N the input to node *N* at the output layer and net^k_j is the input to a node *j* in the k^{th} layer. The learning rate determines what amount of the calculated error sensitivity to weight change will be used for the weight correction. It affects the convergence speed and the stability of weights during learning.

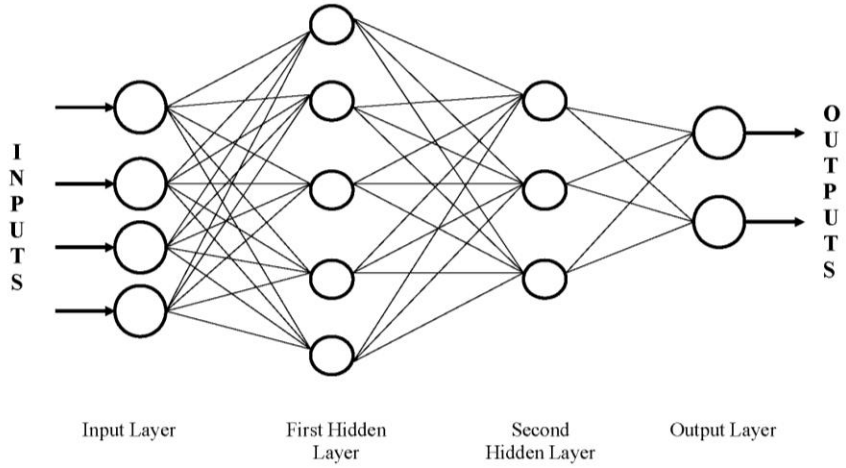

Figure (2): *General configuration of an artificial neural network*

The training process is terminated either when the error between the observed data and the ANN outcomes for all elements in the training set has reached a pre-specified threshold or after the completion of a pre-specified number of learning iterations (epochs).

3. Results and Discussion:

In this study, the suitability of ANN to predict experimental results at different locations will be investigated. The coordinates x and r will be used as the input parameters to the ANN while the mean velocities W will be the output from the network.
The Neurosolution-5 software [12] was used to construct, train and test the networks. In each case, the network was trained using all but one of the velocity distributions obtained experimentally at different values of the coordinate *x*. The network was then required to predict the velocity profile it was not trained for. The predictions obtained were then compared to the experimental results at this coordinate. Once assured that the predictions obtained are reliable, the network could be used in the future to predict the velocity profile at any coordinate *x* for which experimental results do not exist. Since the ANN cannot be accurately used to predict results outside the area of training, predicting the velocity profiles at *x/H* = 0.38 and *x/H* = 18 was not attempted. To evaluate the accuracy of the neural network, the correlation coefficient (*cc*) and the normalized mean square error (*NMSE*) were defined and calculated as:

$$CC = \frac{\sum_{i=1}^{n}[(u_{ANN}^{i}-\bar{u}_{ANN})(u_{exp}^{i}-\bar{u}_{exp})]}{\sqrt{\sum_{i=1}^{n}(u_{ANN}^{i}-\bar{u}_{ANN})^2}\sqrt{\sum_{i=1}^{n}(u_{exp}^{i}-\bar{u}_{exp})^2}} \quad (3)$$

$$NMSE = \frac{n\sum_{i=1}^{n}(u_{exp}^{i}-u_{ANN}^{i})^2}{n\sum_{i=1}^{n}(u_{exp}^{i})^2-(\sum_{i=1}^{n}u_{exp}^{i})^2} \quad (4)$$

where u^{i}_{exp} are the values of the experimental values for the velocity *u* at each coordinate (x_i, r_i), u^{i}_{ANN} are the value the velocity at the same coordinate (x_i, r_i) as predicted by the neural

network, $\bar{u}_{exp}$ and $\bar{u}_{ANN}$ are the average experimental and predicted velocities; respectively and n is the number of data points in the velocity profile at a specific coordinate x_i. Table 1 shows *cc* and *NMSE* obtained for each of the velocity profiles considered.

The velocity distributions at various values of the distance x can be graphically represented. Fig. 3 shows the experimental and predicted velocity distributions for the case under consideration. These preliminary results show that ANN can be used to accurately predict the swirl flow velocity field distribution. Figure 3 shows the normalized swirl mean velocity profiles at x / H = 0.38, 1, 2, 3, 4, 5, 6, 8, 10, 12, 15, and 18; respectively. They show that swirling jet flow velocity characteristics is similar to the free vortex flow in the near field and excluding the region close to the combustor centerline. In general, the flow near the centerline behaves as a forced vortex, while far downstream and away from the

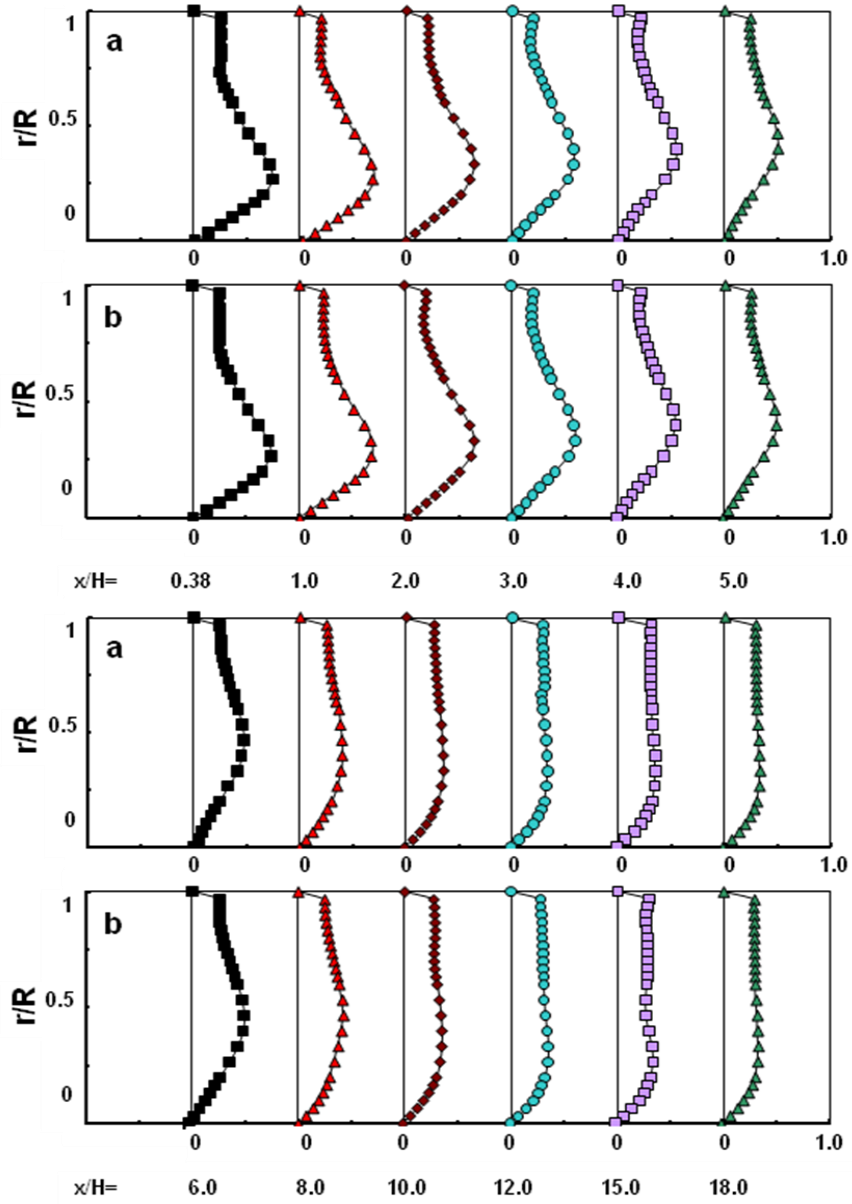

Figure (3): *Evolution of non-dimensional tangential velocity profiles. Top set has near field and bottom set has mid and far field results. (a) Experimental (b) ANN*

Centerline, the tangential velocity is approximately constant over a large area of the combustor's cross-section. As expected, the tangential velocity distribution is asymmetric and its values at the centerline are zeros, while the axial and radial velocity distributions are symmetric (the results are not shown here due to the paper's size limitation).

A comparison between the experimental data and ANN data reveals that the normalized mean square errors (NMSE) are insignificant and the correlation coefficient (CC) is approximately one. These observations are obvious from the results reported in Table 1 as well as Figure 3. The results are encouraging to continue experimenting with the other components of velocities V and U as well as all the normal and shear stresses of all velocity components (their results are not shown here due to the paper's size limitation).

Table (1): *CC and NMSE values as a function of x/H for W profiles.*

x/H	cc	NMSE	x/H	cc	NMSE
.38			6.0	0.9984	0.01167
1.0	0.9927	0.01552	8.0	0.9930	0.01701
2.0	0.9929	0.01551	10.	0.9948	0.01280
3.0	0.9987	0.00371	12.	0.9937	0.02341
4.0	0.9947	0.01378	15.	0.9882	0.07274
5.0	0.9959	0.01128	18.		

4. Conclusions:

A two component LDV system was utilized to measure the flow field turbulence characteristics of a free vortex swirler. As a result, a database of the flow field statistics was established over a fairly wide region downstream of the step. This detailed information should be of value for further development of turbulence models.

This pilot study shows the suitability of the ANN as a method for predicting swirl flow velocity-field reconstruction. More work is underway to show the applicability to other velocity components as well as the effect of the ANN architecture on the predicted values.

5. References:

[1] Gupta, A. K. and Lilley, D. G., *Flowfield Modeling and Diagnostics,* Abacus Press, Tunbridge Wells, UK, 1985.

[2] Dong, M. and Lilley, D. G., *Inlet velocity profile effects on turbulent swirling flow predictions*. J Propul. Power*,* 10 (2), 155-160, 1994.

[3] Goulard, S., Mellor, A. M. and Bilger, R. W., *Combustion measurements in air breathing propulsion engines: survey and research needs*. Combustion Science Tech., 14, 195-201, 1976.

[4] Jones, W. P. and Whitelaw, J. H., *Calculation methods for reacting turbulent flow, a review*. Combustion Flame*,* 48, 1-26, 1982.

[5] So, R. M., Ahmed, S. A. and Mongia, H. C., *An experimental investigation of gas jets in confined swirling air flow*. NASA CR 3832, 1984.

[6] Ahmed, S.A., and Nejad, A.S., *Velocity Measurements in a Research Combustor. Part I. Isothermal Swirling Flow*, Experimental Thermal and Fluid Science Journal, Vol. 5, P. 162-174, 1992.
[7] Pruvost, J., Legrand, J., and Legentilhomme, P., *Three dimensional swirl flow velocity-field reconstruction using a neural network with radial basis function*, Journal of Fluids Engineering, Vol. 123, P. 920-927, 2001.
[8] Ghorbanian, K., Soltani, M.R., Morad, M.R., and Ashjaee, M., *Velocity field recognition in the mixing region of swirl sprays using general regression neural networks*, Journal of Fluids Engineering, Vol. 127, P. 14-23, 2005.
[9] Kartalopoulos, SV., *Understanding neural networks and fuzzy logic: basic concepts and applications*, IEEE Press, 1996.
[10] Skapura, D., *Building neural networks*, New York: ACM Press, Addison-Wesley.
[11] Schalkoff, RJ., *Artificial neural networks*, McGraw-Hill, 1997.
[12] *Neurosolutions 5 software*, www.nd.com, 2005:

Nomenclatures:

H	Step height, mm
R	Combustor radius, mm
S	Swirl number
U, V, W	Mean velocity components, in x, r, and directions, m/s
U_o	Mean axial velocity, upstream of the swirler, m/s
ξ, ρ, θ	Axial, radial, and azimuthal coordinates; respectively, mm, mm, degrees
ρ	Flow density, kg/m^3
ΔY	Uncertainty in velocity U, m/s
μ	Dynamic viscosity, Pa.s